Measurement of microtubule dynamics by spinning disk microscopy in monopolar mitotic spindles
--Manuscript Draft--

Article Type:	Invited Methods Article - JoVE Produced Video
Manuscript Number:	JoVE60478R2
Full Title:	Measurement of microtubule dynamics by spinning disk microscopy in monopolar mitotic spindles
Section/Category:	JoVE Biology
Keywords:	Microtubule dynamics; microtubule growth; plus-end microtubule tracking; prophase; Live cell imaging; spinning disk confocal microscopy
Corresponding Author:	L Dr. Pardo Max-Planck-Institut für experimentelle Medizin Göttingen, Niedersachsen GERMANY
Corresponding Author's Institution:	Max-Planck-Institut für experimentelle Medizin
Corresponding Author E-Mail:	pardo@em.mpg.de
Order of Authors:	Naira Movsisyan
	L Dr. Pardo
Additional Information:	
Question	**Response**
Please indicate whether this article will be Standard Access or Open Access.	Standard Access (US$2,400)
Please indicate the **city, state/province, and country** where this article will be **filmed**. Please do not use abbreviations.	Göttingen, Niedersachsen, Germany

1 **TITLE:**
2 **Measurement of Microtubule Dynamics by Spinning Disk Microscopy in Monopolar Mitotic**
3 **Spindles**
4
5 **AUTHORS AND AFFILIATIONS:**
6 Naira Movsisyan[1,2], Luis A. Pardo[1]
7
8 [1]AG Oncophysiology. Max-Planck Institute of Experimental Medicine, Göttingen, Germany
9 [2]Göttingen Graduate School for Neurosciences, Biophysics, and Molecular Biosciences (GGNB),
10 Göttingen, Germany
11
12 **Corresponding Authors:**
13 Naira Movsisyan   (movsisyan@em.mpg.de)
14 Luis A. Pardo   (pardo@em.mpg.de)
15
16 **KEYWORDS:**
17 microtubule dynamics, microtubule growth, plus-end microtubule tracking, prometaphase, live-
18 cell imaging, spinning disk confocal microscopy
19
20 **SUMMARY:**
21 Here we present a robust and detailed method of microtubule dynamics analysis in cells
22 synchronized in prometaphase using live-cell spinning disk confocal microscopy and MATLAB-
23 based image processing.
24
25 **ABSTRACT:**
26 We describe a modification of an established method to determine microtubule dynamics in
27 living cells. The protocol is based on the expression of a genetically encoded marker for the
28 positive ends of microtubules (EB3 labelled with tdTomato fluorescent protein) and high-speed,
29 high-resolution, live-cell imaging using spinning disk confocal microscopy. Cell cycle
30 synchronization and increased density of microtubules are achieved by inhibiting centrosomal
31 separation in mitotic cells, and analysis of growth is performed using open-source U-Track
32 software. The use of a bright and red-shifted fluorescent protein, in combination with the lower
33 laser power and reduced exposure time required for spinning disk microscopy reduce
34 phototoxicity and the probability of light-induced artifacts. This allows for imaging a larger
35 number of cells in the same preparation while maintaining the cells in a growth medium under
36 standard culture conditions. Because the analysis is performed in a supervised automatic fashion,
37 the results are statistically robust and reproducible.
38
39 **INTRODUCTION:**
40 Microtubules (MTs) are highly dynamic structures found in virtually all eukaryotic cells and in
41 some bacteria[1]. Together with actin and intermediate filaments, they sculpt the cytoskeleton[2,3].
42 Cell division[4], molecule transport[5], flagellar beating[6], the sensation of the surrounding
43 environment through primary cilium[7], hearing (kinocilium)[8,9], embryogenesis[10–12], invasion and
44 metastasis[13,14], and even memory formation[15–18], and many other processes primarily rely on

45 MTs. Participation of MTs in all these events would be impossible without their remarkable ability
46 to rapidly switch between growth (polymerization) and shrinkage (depolymerization). This
47 property is described as dynamic instability[19]. MT dynamicity is altered in many pathological
48 conditions[20–22]. Hence, determining the nature of this property can help to understand disease
49 mechanisms and subsequently their treatment.
50
51 A long list of methods has been developed for MT dynamics analysis, most of which are based on
52 imaging techniques[23]. Initially, wide field light microscopes were used for observing the
53 formation of tubulin polymers in vitro[24]. The discovery of end-binding (EB)-proteins that collect
54 at MT plus-ends and the development of methods to fluorescently label proteins made it possible
55 to observe the behavior of MTs directly in living cells with wide field and confocal fluorescence
56 microscopes[25–27]. One EB-protein is end-binding protein 3 (EB3)[28]; by overexpressing and tracking
57 EB3 fused to a fluorescent protein, MT plus-end assembly rates can be determined[29,30].
58
59 Confocal laser scanning fluorescence microscopy (CLSM) is frequently used to follow MT
60 dynamics. However, this imaging technique poses a high risk of phototoxicity and
61 photobleaching, two undesirable processes for live cell and dim sample imaging[31]. In order to
62 obtain a better signal-to-noise ratio, the laser power and the exposure duration should be high
63 enough while not damaging the samples, and this requires sacrificing resolution in exchange for
64 speed. A suitable alternative to CLSM is spinning disk microscopy[32]. This imaging modality is
65 based on the use of a Nipkow disk[33], which consists of a moving disk bearing an array of pinholes,
66 and works equivalently to many CLS microscopes imaging the same sample simultaneously[34].
67 Therefore, the light from the laser will illuminate several regions in the sample simultaneously
68 but retain the confocal nature. The Nipkow disk, therefore, allows obtaining images similar to
69 CLSM but faster and using less laser power. The Nipkow disk was further improved by Yokogawa
70 Electric, which introduced a second disk with an array of microlenses on it that individually direct
71 light into a respective pinhole, further reducing phototoxicity and photobleaching[35]. Thus,
72 spinning disk laser scanning microscopy became a method of choice for live cell imaging, and it
73 makes it possible to obtain images with high signal-to-noise ratio at a high speed[31,36], which is
74 crucial for resolving signals such as those from the fast-growing MT ends.
75
76 MT dynamics differ temporarily. For example, the mitotic MTs are more dynamic than the
77 interphase ones[37,38]. Similarly, differences in the growth rate and shrinkage have been observed
78 even within the same cell cycle phase, such as mitosis[39,40]. Therefore, to avoid false data
79 collection, the measurement of MT dynamics should be limited to a narrow time-window during
80 the cell cycle. For example, measurement of MT dynamics in prometaphase can be achieved by
81 treating the cells with dimethylenastron (DME), a monastrol analogue that inhibits the motor
82 kinesin Eg5[41] and prevents the formation of the bipolar mitotic spindle[42]. Inhibition of cells at
83 prometaphase with Eg5 inhibitor DME and other monastrol derivatives does not affect the MT
84 dynamics[43–45], which makes DME a useful tool for studying MT dynamics both in fixed and live
85 cells[44].
86
87 Here we combine the method of MT dynamics analysis in prometaphase cells described by Ertych
88 et al.[44] with dual spinning disk imaging. This method allows measurement of the MT dynamics in

89   prometaphase cells collected from a single focal plane with a higher imaging rate, yet without
90   photobleaching and minimal phototoxicity. Furthermore, as a fluorescent reporter, we use
91   tandem dimer Tomato fluorescent protein (tdTomato) which has improved brightness and
92   photostability in comparison to the green fluorescent protein (EGFP) and is excited with lower
93   energy light[46]. Therefore, tdTomato requires less laser power for excitation and is less phototoxic.
94   Altogether, we further improve the method by reducing the phototoxicity and improving the
95   resolution and postprocessing required for the MT dynamics analysis. Additionally, we create a
96   basis for future modifications of the method by combining it with other synchronization
97   techniques.

PROTOCOL:

1.   Seeding of HeLa cells

1.1.   Prepare 2 mL of 5 µg/mL fibronectin solution in phosphate buffered saline (PBS) and add
450 µL of it into each well of a 4 well chambered coverslip (#1.5). Incubate the slide for 15 min at
37 °C and 5% CO_2.

1.2.   Rinse asynchronously growing HeLa cells with Dulbecco's Phosphate Buffered Saline
(DPBS) and incubate with trypsin-EDTA (0.05%: 0.02%; w:v) for 5 min at 37 °C. Stop the enzymatic
reaction by the addition of Roswell Park Memorial Institute (RPMI) 1640 medium supplemented
with 10% heat-inactivated fetal calf serum (FCS) at 3:1 (v:v) ratio of added trypsin-EDTA.

NOTE: HeLa cells were maintained in RPMI 1640 medium supplemented with 10% heat-
inactivated FCS at 37 °C and 5% CO_2 and were routinely passaged once they reached 80–90%
confluency as described above.

1.3.   Determine the cell concentration using a Neubauer chamber. Mix a 50 µL aliquot of the
cell suspension with trypan blue at 1:1 (v:v) ratio, resuspend, and transfer 10 µL of the suspension
into the chamber. Count only the trypan blue-negative cells inside of the four large squares (for
details see Phelan et al.[47]). Derive the cell concentration from the counted cell number using the
following formula:

$$\text{Concentration (cells/mL)} = \frac{(\text{number of cells} \times \text{dilution factor} \times 10{,}000)}{\text{number of squares}}$$

1.4.   Pellet the cells by centrifugation at 300 x g for 2 min. Resuspend with fresh RPMI 1640 in
order to obtain 1×10^6 cells/mL.

1.5.   Remove the fibronectin from the chambered coverslip, wash the wells twice with DPBS,
and seed 50,000 cells per well.

1.6.   Return the chambered coverslip with the cells to the incubator and grow them for 24 h at
37 °C and 5% CO_2.

2.   Expression of pEB3-tdTomato in HeLa cells.

2.1.   Prepare a 1.5 mL microcentrifuge tube. For each tube, dilute 2 µg of pEB3-tdTomato[48] with transfection buffer (synthetic product in aqueous solution) to a final volume of 396 µL.

2.2.   Add 4 µL of transfection reagent (non-lipidic, containing polyethylenimine) to the first tube, and vortex the mixture immediately for exactly 10 s.

2.3.   Briefly spin down the tube with a microcentrifuge and incubate at room temperature (RT) for 10 min.

2.4.   Remove the HeLa cells from the incubator. Dropwise, add 100 µL of the transfection mixture to each well of a 4 well chambered coverslip, and return the cells to the incubator.

2.5.   After 4 h of incubation at 37 °C and 5% CO_2, supplement the cells with fresh growth medium and incubate for at least 24 h at 37 °C and 5% CO_2.

NOTE: It is necessary to optimize transfection conditions for each cell type. The expression levels need to be low enough to allow the identification of single MT growing ends. Alternatively, a cell line stably expressing EB3-tdTomato can be used in the experiments; this would reduce variability in expression levels of EB3-tdTomato between preparations and between cells from the same preparation[49].

3.   Synchronization and live-cell imaging of pEB3-tdTomato–expressing HeLa cells.

3.1.   Prepare a 2.5 µM solution of dimethylenastron (DME) in phenol-red free Dulbecco's Modified Eagle Medium (DMEM) supplemented with 10% FCS and 2 mM L-glutamine or an alternative glutamine supply.

3.2.   Replace the growth medium in the chambered coverslip with 500 µL of the growth medium containing 2.5 µM DME and incubate the cells at 37 °C and 5% CO_2.

3.3.   After 3.5 h of incubation with DME, transfer the cells to the microscope, mount the chambered coverslip into an environmental chamber with dark panels for imaging at 37 °C and 5% CO_2, and further incubate until the total incubation time is 4 h.

NOTE: The maintenance of the temperature at 37 °C without fluctuation is crucial for the experiment.

3.4.   Perform the time-lapse imaging on an inverted microscope equipped with a 100x 1.49 N.A. oil immersion objective, a dual spinning disk confocal system, and a reliable autofocus system for continuous maintenance of the focal plane. Define the imaging parameters as follows.

176   NOTE: We use an Electron Multiplying Charge-Coupled Device camera (EM-CCD).

177

178   3.4.1. For EB3-tdTomato excitation, use a 561 nm laser line with 200 ms exposure time. Collect
179   the emitted light through a quadruple bandpass (405, 488, 561, 640 nm) dichroic mirror and a
180   600/52 nm emission filter.

181

182   NOTE: Laser power can be adjusted for each imaged cell to prevent image saturation. In all time-
183   lapse movies given here the laser power was set to 5.3 mW.

184

185   3.4.2. Find a cell in prometaphase and focus in the Z-plane corresponding to the center of the
186   monopolar mitotic spindle. Acquire images every 0.5 s over a total of 1 min with no binning and
187   no illumination between the exposures.

188

189   **4.   Analysis of the MT dynamics using U-Track v2.2.0**

190

191   4.1.   To analyze the MT dynamics a numerical computing environment software is required
192   (e.g., MATLAB).

193

194   NOTE: Basic understanding of the software is sufficient for the analysis. Comprehensive help
195   material   and   tutorials   are   available   on   the   developer's   website
196   (https://uk.mathworks.com/products/matlab/getting-started.html).

197

198   4.2.   Download (https://github.com/DanuserLab/u-track) and install the open-source U-Track
199   v2.2.0 software following the detailed instructions given in the "Readme_u-track.pdf" file[50–52].

200

201   4.3.   Launch the numerical-analysis software and add U-Track v2.2.0 folder with subfolders
202   into the software search path.

203

204   4.4.   From the command window call "**movieSelectorGUI**". This opens a dialogue window from
205   which the raw files generated by the image acquisition software at the microscope can be
206   imported (**Supplementary Figure 1**, **Figure 2**, **Figure 3**, **Figure 4**).

207

208   NOTE: The U-Track software is compatible with other image data formats. It uses Bio-Formats,
209   which recognizes different life science data formats[53].

210

211   4.5.   The size of each image is read from the metadata automatically. Manually enter the
212   numerical aperture of the objective (in this case 1.49) and the time interval (0.5 s) used for
213   imaging (**Supplementary Figure 1B**). Additionally, information on the excitation wavelength, the
214   fluorophore, and the exposure time can also be provided, but they are not critical for further
215   analysis.

216

217   4.6.   Once all the images are loaded, save the entered time-lapse series as a movie list by
218   selecting the "**Save As Movie List**". On the right side of the dialogue window select the "**U-Track**"
219   option and press "**Continue**" (**Supplementary Figure 1C**).

NOTE: The values are optimized for HeLa cells. If switching to a different cell line, the values should be defined again. Alternatively, use the settings recommended by the software developers. The detailed explanation of each of the parameters and how they should be defined can be found in the technical report provided with the previous version of the software, plusTipTracker[50].

4.7.   From the pop-up window select "**Microtubule Plus-Ends**" and press "**Ok**" (**Supplementary Figure 1C**). The new dialogue window allows determining the parameters for the three steps of the analysis (**Supplementary Figure 1D**), which are detection, tracking, and track analysis.

4.8.   In step 1 choose "**Settings**" and from a drop-down menu select "**Comet Detection**" as a detection method (**Supplementary Figure 2B**).

4.8.1. From the new dialogue window define the parameters for the difference of Gaussians filter and the watershed segmentation as follows (**Supplementary Figure 2C**): Mask process to be used for the detection = None; Low-pass Gaussian standard deviation = 1 pixel; High-pass Gaussian standard deviation = 3 pixels; Minimum threshold = 3 standard deviations; Threshold step size = 0.25 standard deviations. Select "**Apply Settings to All Movies**" and "**Apply**".

4.9.   In step 2, the parameters for linking, gap closing, merging and splitting, and Kalman filter functions are defined in three steps as highlighted in pink, green, and blue, accordingly (**Supplementary Figure 3B**). For these steps, select the "**Microtubule Plus-end Dynamics**" and from the "**Setting**" option define the values as indicated in **Supplementary Figure 3C–E**, respectively.

4.9.1. For problems with dimensionality, choose "2" from the drop-down menu. Use Maximum Gap to Close = 5 frames; Minimum Length of Track Segments from First Step =3 frames. As before, select "**Apply Settings to All Movies**" and click on "**Apply**".

4.10.   In step 3 of the analysis, the detected MT tracks are classified (**Supplementary Figure 4**). As a track analysis method, choose "**Microtubule Dynamics Classification**" and define the parameters through the "**Setting**" button as indicated in **Supplementary Figure 4B,C**. After that, choose the "**Apply Settings to All Movies**" box and click on "**Apply**".

4.11.   Once all the parameters are defined, from the "**Control Panel–U-Track**" window (**Supplementary Figure 1D**) select the "**Apply Check/Uncheck to All Movies**" and "**Run All Movies**" boxes and press "**Run**". This will initiate the MT analysis of the time-lapse series.

4.12.   Once the movie processing is completed, a message "Your movie(s) have been processed successfully" is displayed. Press "**Ok**", then "**Save**".

4.13.   Now it is safe to quit the numerical-analysis software. The results from the movie

264 processing are stored in subfolder structures as m-files in the folder where the raw files are
265 stored.
266
267 **5.   Statistical analysis of the MT dynamics**
268
269 5.1.   Import the m-files into a preferred statistic analysis program.
270
271 NOTE: In our case, we first import the files in a standard spreadsheet to make them readable.
272 The m-files contain statistical information (median, mean, and standard deviation) on different
273 parameters (e.g., growth speed, MT dynamicity). The detailed list of the parameters is given in
274 the technical report provided with the previous version of the software, plusTipTracker[50,52]. The
275 generated m-files can also be imported into other data processing software.
276
277 5.2.   Choose the "growth speed mean" parameter and import it into a table for statistics and
278 display. Enter the information on other parameters, (e.g., "dynamicity") either in a new table or
279 in a new column of the same grouped table and plot.
280
281 **REPRESENTATIVE RESULTS:**
282 Following the given protocol outlined in **Figure 1A**, the pEB3-tdTomato plasmid was transiently
283 expressed in asynchronously growing HeLa cells. The cells were synchronized 48 h after the
284 transfection at prometaphase through DME treatment (**Figure 1B**). This step ensured that the
285 measurement of MT dynamics was always done at the same phase of the cell cycle. The time-
286 lapse movies were further processed and analyzed with U-Track v2.2.0 as described in its
287 supplementary documentation[50–52]. Although the plus-end binding proteins trace only MT
288 growth phases, the U-Track v2.2.0 extrapolates the information on the pause and shrinkage
289 events by linking sequential growth phases and reconstructing the full trajectories[26,50]. The
290 algorithm is based on the spatially and temporally global tracking framework described by
291 Jaqaman et al.[51].
292
293 It is important to note that the sensitivity and accuracy of the analysis are strongly dependent on
294 several analysis parameters. As an example, the time-lapse movies were analyzed as described
295 in the protocol (**Figure 1C**, Video 1 "Before", and Video 2 "After" the analysis), and the resulting
296 growth speed and dynamicity (collective displacement of gap-containing tracks over their entire
297 lifetime) are plotted in **Figure 1E,F**, respectively (black circles). Then the parameters described to
298 greatly affect the analysis[50], such as "Maximum Gap Length" and "Maximum Shrinkage Factor"
299 were modified for the same set of time-lapse movies (Videos 3 and 4, respectively). The
300 corresponding values of growth speed and dynamicity are given in **Figure 1E,F** as red squares and
301 blue triangles, respectively. The resulting growth speed was not deeply affected. However, the
302 values obtained for dynamicity were significantly different when "Maximum Gap Length" was
303 modified, while it remained unchanged upon altering the "Maximum Shrinkage Factor". As
304 shown in **Figure 1D**, in all three cases the detection of the MT subtracks was similarly robust. Yet,
305 the reconstruction of the full MT trajectories was mostly affected when "Maximum Gap Length"
306 was set to 15 (**Figure 1D**, inset images). Further, in order to assess whether the imaging
307 conditions interfered with the MT behavior, the first (1–61 frames) and the second (61–121

308   frames) halves of the time-lapse series were analyzed separately and the corresponding growth
309   speed and dynamicity values were compared (**Figure 1G,H**, respectively). As expected, no
310   significant differences were detected between the two parts of the time-lapse series. In videos
311   1–8 time-lapse images of a mitotic cell synchronized in prophase and expressing EB3-tdTomato
312   are given (duration = 1 min; interval = 0.5 s).
313
314   **FIGURE AND TABLE LEGENDS:**
315   **Figure 1: Analysis of the MT dynamics in HeLa cells synchronized in prometaphase**. (**A**) An
316   outline of the steps of the protocol. (**B**) The schematic representation of the mechanism of DME
317   mediated formation of a monopolar mitotic spindle. (**C**) A montage of the first 10 frames of the
318   time-lapse movie processed with U-Track software with every second frame shown. The detected
319   trajectories of the MT growth are marked with red. (**D**) The time series projection of the raw
320   image file and after MT tracking using the settings described in the protocol ("optimal"), and
321   when changing either "Maximum Gap Length" or "Maximum Shrinkage Factor" are given. The
322   insets represent the full MT trajectories, which consist of the growth (red), pause (light blue),
323   shrinkage (yellow), fgap reclassified as growth (green) and bgap reclassified as pause (dark blue)
324   events. The growth speed means (**E**) and the dynamicity (**F**) values are shown, and the results
325   using either of the suggested optimal criteria (black circles), maximal gap length set to 15 (red
326   squares), or the maximal shrinkage factor set to 1.0 (blue triangles) are plotted (n = 45 cells; mean
327   ± SEM; one-way ANOVA analysis with Tukey post hoc test for multiple comparison). The growth
328   speed means (**G**) and the dynamicity (**H**) values are shown for the first (1–61 frames) and second
329   (61–121 frames) halves of the time-lapse movies (n = 45 cells; mean ± SEM; unpaired t-test with
330   Welch's correction).
331
332   **Video 1. A representative time-lapse raw image of a prometaphase cell before the analysis.**
333
334   **Video 2**. **Detection and tracking of the MTs in a cell in Video 1 using the suggested settings for**
335   **U-Track software.** The same time-lapse image in Video 1 processed with U-Track v2.2.0 software
336   using the described settings, and the detected growth tracks are marked in red.
337
338   **Video 3. Detection and tracking of the MTs in a cell in Video 1 using a nonoptimal value for the**
339   **"Maximum Gap Length".** The same time-lapse image in Video 1 processed with U-Track v2.2.0
340   software using the same settings as before, but with the "Maximum Gap Length" set to 15. The
341   rest of the parameters were not altered.
342
343   **Video 4. Detection and tracking of the MTs in a cell in Video 1 using a nonoptimal value for the**
344   **"Maximum Shrinkage Factor".** The same time-lapse image in Video 1 processed with U-Track
345   v2.2.0 software using the same settings as before, but with the "Maximum Shrinkage Factor" set
346   to 1. The rest of the parameters were not altered.
347
348   **Video 5. An example of a time-lapse series of a cell with cell debris.** After the analysis, some cell
349   debris was also detected by the software during MT tracking.
350
351   **Video 6. Raw data corresponding to Video 5.**

352

353   **Video 7. An example of a time-lapse series of a cell with a high expression of EB3-tdTomato**
354   **resulting in poor definition of growing tips.**

355

356   **Video 8. Raw data corresponding to Video 7.**

357

358   **Supplementary Figure 1. The workflow of the analysis using U-Track software.** (**A**) A schematic
359   of the steps employed by the software. (**B**) A screenshot of the Bio-Formats importer showing
360   how to import the time-lapse files. (**C**) After uploading the files, U-Track with the MT plus-ends
361   module is selected. (**D**) A screenshot of the control panel of U-Track where the settings for comet
362   detection, tracking, and track analysis are defined.

363

364   **Supplementary Figure 2. Description of the first step of the analysis, the comet detection.** (**A**)
365   An outline of the major events performed by the algorithm. (**B**, **C**) Screenshots from the software
366   are given with the optimal values indicated.

367

368   **Supplementary Figure 3. Description of the second step of the analysis, the comet tracking**. (**A**)
369   The main steps performed by the algorithm are outlined. (**B**) A screenshot of the "Tracking" panel
370   is given. The Maximum Gap Close corresponds to the Maximum Gap Length and is set to 5. The
371   tracking of three substeps highlighted with red, green, and blue rectangles. (**C,D,E**) The numerical
372   values necessary for each substep are entered here. The Maximum Shrinkage Factor is set to 1.5
373   as indicated in (**D**).

374

375   **Supplementary Figure 4. Description of the last step of the analysis, track analysis.** (**A**) The MT
376   dynamics classification and reclassification of the compound tracks is performed during this step.
377   (**B,C**) Screenshots of the track analysis and the corresponding settings are shown.

378

379   **DISCUSSION:**
380   Here, we describe a modification of a method first established by Ertych et al.[44]. Along with
381   several other modifications, we combine this technique of MT dynamics analysis with dual
382   spinning disk confocal imaging. The use of the dual spinning disk improves the resolution of
383   growing MTs while reducing phototoxicity[36]. We further reduce the photobleaching and laser
384   light-induced damage of the cells by switching to a longer wavelength fluorescent reporter. The
385   tdTomato fluorescent protein has a higher coefficient of photostability and brightness in
386   comparison to an EGFP[46]. Finally, the measurement of MT dynamics is limited to only one Z-plane
387   due to the limitations of the follow-up analysis with U-Track. The U-Track software is designed to
388   detect the fluorescently-labelled MT tips in an XYZ-axis[50,51]. Therefore, taking a Z-stack time-lapse
389   series and creating maximal projection time-lapse series is prone to generate false results. Signals
390   detected in different Z-planes and not belonging to the same growing MT are brought together
391   in the maximal projection, thus creating a false trajectory of MT growth.

392

393   The synchronization protocol used here induces a high density of MTs by restricting the mitotic
394   spindle to a monopolar structure. The mitotic MTs are highly dynamic structures with phases of
395   growth and shrinkage, with a pause at the transition between them[19,54,55]. Due to the high density

396　of the growing MTs, detection of the pause events followed by either shrinkage or growth is
397　prone to false results if the tracking parameters are set incorrectly. The U-Track software tracking
398　modules detect so-called subtracks (episodes of continuous growth) and then classifies them as
399　compound tracks with pause events termed "gaps". Applegate et al. discuss two parameters
400　critical for the tracking and subtrack linking[50]. These are "Maximum Gap Length" and "Maximum
401　Shrinkage Factor". If the subtrack being followed reappears in the growing direction of the MT in
402　the subsequent time-steps, then it is classified as a forward gap. On the other hand, if the
403　subtrack reappears opposite to the growth direction, it will be classified as a backward gap. The
404　Maximum Gap Length defines the number of the frames to be searched for the forward and
405　backward gaps. As mentioned, the high density and by nature high dynamicity of the mitotic MTs
406　sets the limitation, and smaller values should be defined. As shown in **Figure 1E** the dynamicity
407　is affected the most. The dynamicity is calculated as collective displacement of all gap-containing
408　tracks over their global lifespans. The second parameter, the Maximum Shrinkage Factor, has
409　little to no effect on either dynamicity or growth speed (**Figure 1D,E**).
410
411　In general, when studying MT growth properties, careful attention should be paid to the imaging
412　conditions. First, the MTs are very sensitive to temperature and depolymerize when exposed to
413　cold growth medium[56–59]. Therefore, to avoid the collection of false results, the temperature
414　should be strictly controlled throughout the entire experiment. Second, the ionic composition of
415　the medium used during the experiments can affect MT growth[58,60]. For example, exposure to
416　calcium ions affects the MT dynamics in different ways[61,62]. Hence, the composition of the growth
417　medium used in all experiments should be the same. Similarly, the parameters of the analysis
418　should be defined once and maintained constant for all the repetitions. Additionally, the time-
419　lapse movies generated after the analysis should be visually inspected, and any movie with
420　background noise giving rise to false positives (Videos 5 and 6) or with high expression of
421　tdTomato resulting in poor resolution of the MT growing tips (Videos 7 and 8) should be excluded
422　from further statistical analysis.
423
424　Recently, the combination of lattice light-sheet microscopy of a mitotic spindles at subsecond
425　intervals, together with sophisticated image processing allows the analysis of MT assembly rates
426　in three dimensions[63,64]. This has obvious advantages over CLSM, but further improvements will
427　be required before the method becomes of general use, such as the expansion of strategies used
428　in U-Track to the third dimension[26,50,63].
429
430　The protocol of MT dynamics detection we describe here can be a method of choice for drug
431　screening. The method is robust, and it successfully removes human bias compared to the
432　analysis performed manually. The automation of the movie processing allows the analysis of
433　thousands of MT tracks within each cell, thus increasing the statistical power of the analysis.
434　Furthermore, the method can be modified by changing, for instance, the synchronization
435　protocol and obtaining cells from different phases of the cell cycle. This can, for example, be a
436　useful tool for screening MT targeting chemotherapeutic drugs when the effect on interphase
437　and dividing cells should be distinguished.
438

445

446 **REFERENCES:**
447 1.   Erickson, H. P. Evolution of the cytoskeleton. *Bioessays.* **29** (7), 668–677 (2007).
448 2.   Pollard, T. D., Goldman, R. D. Overview of the Cytoskeleton from an Evolutionary
449 Perspective. *Cold Spring Harbor Perspectives in Biology.* **10** (7), (2018).
450 3.   Wade, R. H. On and around microtubules: an overview. *Molecular Biotechnology.* **43** (2),
451 177–191 (2009).
452 4.   Forth, S., Kapoor, T. M. The mechanics of microtubule networks in cell division. *Journal of
453 Cell Biology.* **216** (6), 1525–1531 (2017).
454 5.   Franker, M. A., Hoogenraad, C. C. Microtubule-based transport - basic mechanisms, traffic
455 rules and role in neurological pathogenesis. *Journal of Cell Science.* **126** (Pt 11), 2319–2329
456 (2013).
457 6.   Lindemann, C. B., Lesich, K. A. Flagellar and ciliary beating: the proven and the possible.
458 *Journal of Cell Science.* **123** (Pt 4), 519–528 (2010).
459 7.   Wheway, G., Nazlamova, L., Hancock, J. T. Signaling through the Primary Cilium. *Frontiers
460 in Cell and Developmental Biology.* **6**, 8 (2018).
461 8.   Falk, N., Losl, M., Schroder, N., Giessl, A. Specialized Cilia in Mammalian Sensory Systems.
462 *Cells.* **4** (3), 500–519 (2015).
463 9.   Spoon, C., Grant, W. Biomechanical measurement of kinocilium. *Methods in Enzymology.*
464 **525**, 21–43 (2013).
465 10.   Zenker, J. et al. A microtubule-organizing center directing intracellular transport in the
466 early mouse embryo. *Science.* **357** (6354), 925–928 (2017).
467 11.   Goldstein, B. Embryonic polarity: a role for microtubules. *Current Biology.* **10** (22), R820–
468 822 (2000).
469 12.   Uchida, S., Shumyatsky, G. P. Deceivingly dynamic: Learning-dependent changes in
470 stathmin and microtubules. *Neurobiology of Learning and Memory.* **124**, 52–61 (2015).
471 13.   Fife, C. M., McCarroll, J. A., Kavallaris, M. Movers and shakers: cell cytoskeleton in cancer
472 metastasis. *British Journal of Pharmacology.* **171** (24), 5507–5523 (2014).
473 14.   Bouchet, B. P., Akhmanova, A. Microtubules in 3D cell motility. *Journal of Cell Science.* **130**
474 (1), 39–50 (2017).
475 15.   Dent, E. W. Of microtubules and memory: implications for microtubule dynamics in
476 dendrites and spines. *Molecular Biology of the Cell.* **28** (1), 1–8 (2017).
477 16.   Craddock, T. J., Tuszynski, J. A., Hameroff, S. Cytoskeletal signaling: is memory encoded in
478 microtubule lattices by CaMKII phosphorylation? *PLOS Computational Biology.* **8** (3), (2012).
479 17.   Smythies, J. Off the beaten track: the molecular structure of long-term memory: three
480 novel   hypotheses-electrical,   chemical   and   anatomical   (allosteric).   *Frontiers   in
481 Integrative Neuroscience.* **9**, 4 (2015).
482 18.   Kaganovsky, K., Wang, C. Y. How Do Microtubule Dynamics Relate to the Hallmarks of
483 Learning and Memory? *Journal of Neuroscience.* **36** (22), 5911–5913 (2016).

484   19.   Mitchison, T., Kirschner, M. Dynamic instability of microtubule growth. *Nature.* **312**
485   (5991), 237–242 (1984).
486   20.   Dubey, J., Ratnakaran, N., Koushika, S. P. Neurodegeneration and microtubule dynamics:
487   death by a thousand cuts. *Frontiers in Cellular Neuroscience.* **9**, 343 (2015).
488   21.   Parker, A. L., Kavallaris, M., McCarroll, J. A. Microtubules and their role in cellular stress
489   in cancer. *Frontiers in Oncology.* **4**, 153 (2014).
490   22.   Honore, S., Pasquier, E., Braguer, D. Understanding microtubule dynamics for improved
491   cancer therapy. *Cell and Molecular Life Sciences.* **62** (24), 3039–3056 (2005).
492   23.   Straube, A. in *Methods in Molecular Biology*. (Humana Press, Totowa, NJ, 2011).
493   24.   Budde, P. P., Desai, A., Heald, R. Analysis of microtubule polymerization in vitro and during
494   the cell cycle in Xenopus egg extracts. *Methods.* **38** (1), 29–34 (2006).
495   25.   Gierke, S., Kumar, P., Wittmann, T. Analysis of microtubule polymerization dynamics in
496   live cells. *Methods in Cell Biology.* **97**, 15–33 (2010).
497   26.   Matov, A. et al. Analysis of microtubule dynamic instability using a plus-end growth
498   marker. *Nature Methods.* **7** (9), 761–768 (2010).
499   27.   Bailey, M., Conway, L., Gramlich, M. W., Hawkins, T. L., Ross, J. L. Modern methods to
500   interrogate microtubule dynamics. *Integrative Biology (Camb).* **5** (11), 1324–1333 (2013).
501   28.   Galjart, N. Plus-end-tracking proteins and their interactions at microtubule ends. *Current*
502   *Biology.* **20** (12), R528–537 (2010).
503   29.   Stepanova, T. et al. Visualization of microtubule growth in cultured neurons via the use of
504   EB3-GFP (end-binding protein 3-green fluorescent protein). *Journal of Neuroscience.* **23** (7),
505   2655–2664 (2003).
506   30.   Zwetsloot, A. J., Tut, G., Straube, A. Measuring microtubule dynamics. *Essays in*
507   *Biochemistry.* **62** (6), 725–735 (2018).
508   31.   Bayguinov, P. O. et al. Modern Laser Scanning Confocal Microscopy. *Current Protocols in*
509   *Cytometry.* **85** (1), e39 (2018).
510   32.   Nakano, A. Spinning-disk confocal microscopy -- a cutting-edge tool for imaging of
511   membrane traffic. *Cell Structure and Function.* **27** (5), 349–355 (2002).
512   33.   Nipkow, P. Elektrisches teleskop. Germany patent (1884).
513   34.   Yin, S., Lu, G., Zhang, J., Yu, F. T., Mait, J. N. Kinoform-based Nipkow disk for a confocal
514   microscope. *Applied Optics.* **34** (25), 5695–5698 (1995).
515   35.   Tanaami, T., Kenta, M. Nipkow disk for confocal optical scanner. (1992). European patent
516   application EP92114750A.
517   36.   Oreopoulos, J., Berman, R., Browne, M. Spinning-disk confocal microscopy: present
518   technology and future trends. *Methods in Cell Biology.* **123**, 153–175 (2014).
519   37.   Rusan, N. M., Fagerstrom, C. J., Yvon, A. M., Wadsworth, P. Cell cycle-dependent changes
520   in microtubule dynamics in living cells expressing green fluorescent protein-alpha tubulin.
521   *Molecular Biology of the Cell.* **12** (4), 971–980 (2001).
522   38.   Rusan, N. M., Fagerstrom, C. J., Yvon, A.-M. C., Wadsworth, P. Cell Cycle-Dependent
523   Changes in Microtubule Dynamics in Living Cells Expressing Green Fluorescent Protein-α Tubulin.
524   *Molecular Biology of the Cell.* **12** (4), 971–980 (2001).
525   39.   Liu, D., Davydenko, O., Lampson, M. A. Polo-like kinase-1 regulates kinetochore-
526   microtubule dynamics and spindle checkpoint silencing. *Journal of Cell Biology.* **198** (4), 491–499
527   (2012).

528 40.   Maiato, H., Sunkel, C. E. Kinetochore–microtubule interactions during cell division.
529 *Chromosome Research.* **12** (6), 585–597 (2004).
530 41.   Muller, C. et al. Inhibitors of kinesin Eg5: antiproliferative activity of monastrol analogues
531 against human glioblastoma cells. *Cancer Chemotherrapy and Pharmacology.* **59** (2), 157–164
532 (2007).
533 42.   Mayer, T. U. et al. Small molecule inhibitor of mitotic spindle bipolarity identified in a
534 phenotype-based screen. *Science.* **286** (5441), 971–974 (1999).
535 43.   Kapoor, T. M., Mayer, T. U., Coughlin, M. L., Mitchison, T. J. Probing spindle assembly
536 mechanisms with monastrol, a small molecule inhibitor of the mitotic kinesin, Eg5. *The Journal*
537 *of Cell Biology.* **150** (5), 975–988 (2000).
538 44.   Ertych, N. et al. Increased microtubule assembly rates influence chromosomal instability
539 in colorectal cancer cells. *Nature Cell Biology.* **16** (8), 779–791 (2014).
540 45.   Brito, D. A., Yang, Z., Rieder, C. L. Microtubules do not promote mitotic slippage when the
541 spindle assembly checkpoint cannot be satisfied. *The Journal of Cell Biology.* **182** (4), 623–629
542 (2008).
543 46.   Shaner, N. C., Patterson, G. H., Davidson, M. W. Advances in fluorescent protein
544 technology. *Journal of Cell Science.* **120** (24), 4247–4260 (2007).
545 47.   Phelan, M. C., Lawler, G. Cell Counting. *Current Protocols in Cytometry.* **00** (1), A.3A.1–
546 A.3A.4, (1997).
547 48.   Merriam, E. B. et al. Synaptic regulation of microtubule dynamics in dendritic spines by
548 calcium, F-actin, and drebrin. *Journal of Neuroscience.* **33** (42), 16471–16482 (2013).
549 49.   Samora, C. P. et al. MAP4 and CLASP1 operate as a safety mechanism to maintain a stable
550 spindle position in mitosis. *Nature Cell Biology.* **13** (9), 1040–1050 (2011).
551 50.   Applegate, K. T. et al. plusTipTracker: Quantitative image analysis software for the
552 measurement of microtubule dynamics. *Journal of Structural Biology.* **176** (2), 168–184 (2011).
553 51.   Jaqaman, K. et al. Robust single-particle tracking in live-cell time-lapse sequences. *Nature*
554 *Methods.* **5** (8), 695–702 (2008).
555 52.   Stout, A., D'Amico, S., Enzenbacher, T., Ebbert, P., Lowery, L. A. Using plusTipTracker
556 Software to Measure Microtubule Dynamics in Xenopus laevis Growth Cones. *Journal of*
557 *Visualized Experiments.* e52138 (2014).
558 53.   Linkert, M. et al. Metadata matters: access to image data in the real world. *The Journal of*
559 *Cell Biology.* **189** (5), 777–782 (2010).
560 54.   Brouhard, G. J. Dynamic instability 30 years later: complexities in microtubule growth and
561 catastrophe. *Molecular Biology of the Cell.* **26** (7), 1207–1210 (2015).
562 Burbank, K. S., Mitchison, T. J. Microtubule dynamic instability. *Current Biology.* **16** (14), R516–
563 517 (2006).
564 55.   Caplow, M., Shanks, J., Ruhlen, R. L. Temperature-jump studies of microtubule dynamic
565 instability. *Journal of Biological Chemistry.* **263** (21), 10344–10352 (1988).
566 56.   Prasad, V., Jordan, M. A., Luduena, R. F. Temperature sensitivity of vinblastine-induced
567 tubulin polymerization in the presence of microtubule-associated proteins. *Journal of Protein*
568 *Chemistry.* **11** (5), 509–515 (1992).
569 57.   Wasteneys, G. O. Microtubules Show their Sensitive Nature. *Plant and Cell Physiology.* **44**
570 (7), 653–654 (2003).
571 58.   Turi, A., Lu, R. C., Lin, P.-S. Effect of heat on the microtubule disassembly and its

relationship to body temperatures. *Biochemical and Biophysical Research Communications.* **100** (2), 584–590 (1981).

59.   Safinya, C. R. et al. The effect of multivalent cations and Tau on paclitaxel-stabilized microtubule assembly, disassembly, and structure. *Advances in Colloid and Interface Science.* **232**, 9–16 (2016).

60.   Sandoval, I. V., Weber, K. Calcium-Induced Inactivation of Microtubule Formation in Brain Extracts. *European Journal of Biochemistry.* **92** (2), 463–470 (1978).

61.   Vater, W., Böhm, K. J., Unger, E. Tubulin assembly in the presence of calcium ions and taxol: Microtubule bundling and formation of macrotubule—ring complexes. *Cell Motility.* **36** (1), 76–83 (1997).

62.   Yamashita, N. et al. Three-dimensional tracking of plus-tips by lattice light-sheet microscopy permits the quantification of microtubule growth trajectories within the mitotic apparatus. *Journal of Biomedical Optics.* **20** (10), 1–18, 18 (2015).

63.   Pamula, M. C. et al. High-resolution imaging reveals how the spindle midzone impacts chromosome movement. *Journal of Cell Biology.* **218** (8), 2529–2544 (2019).
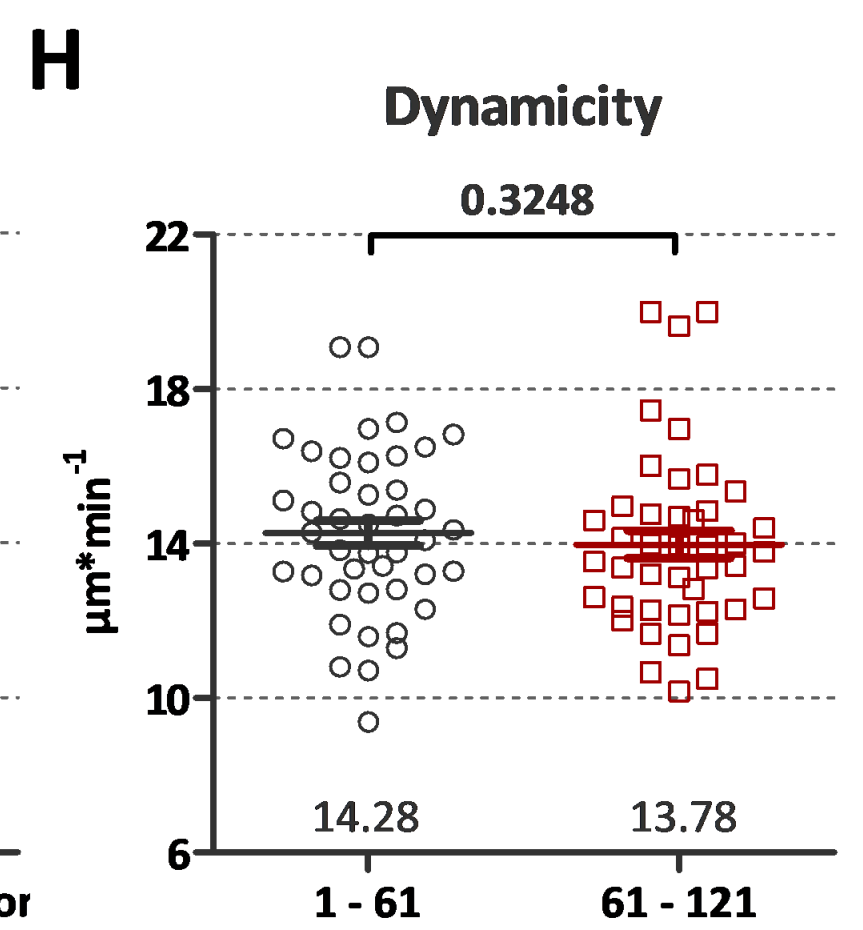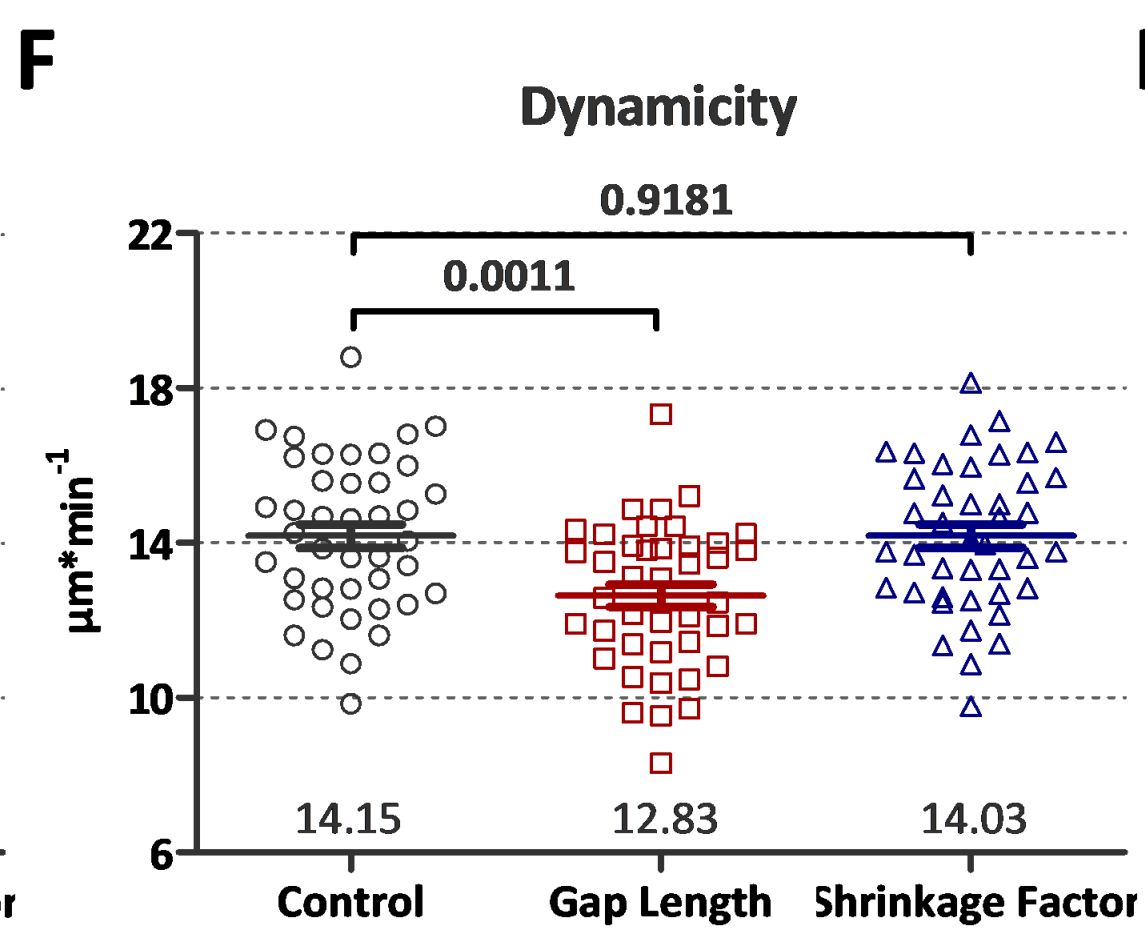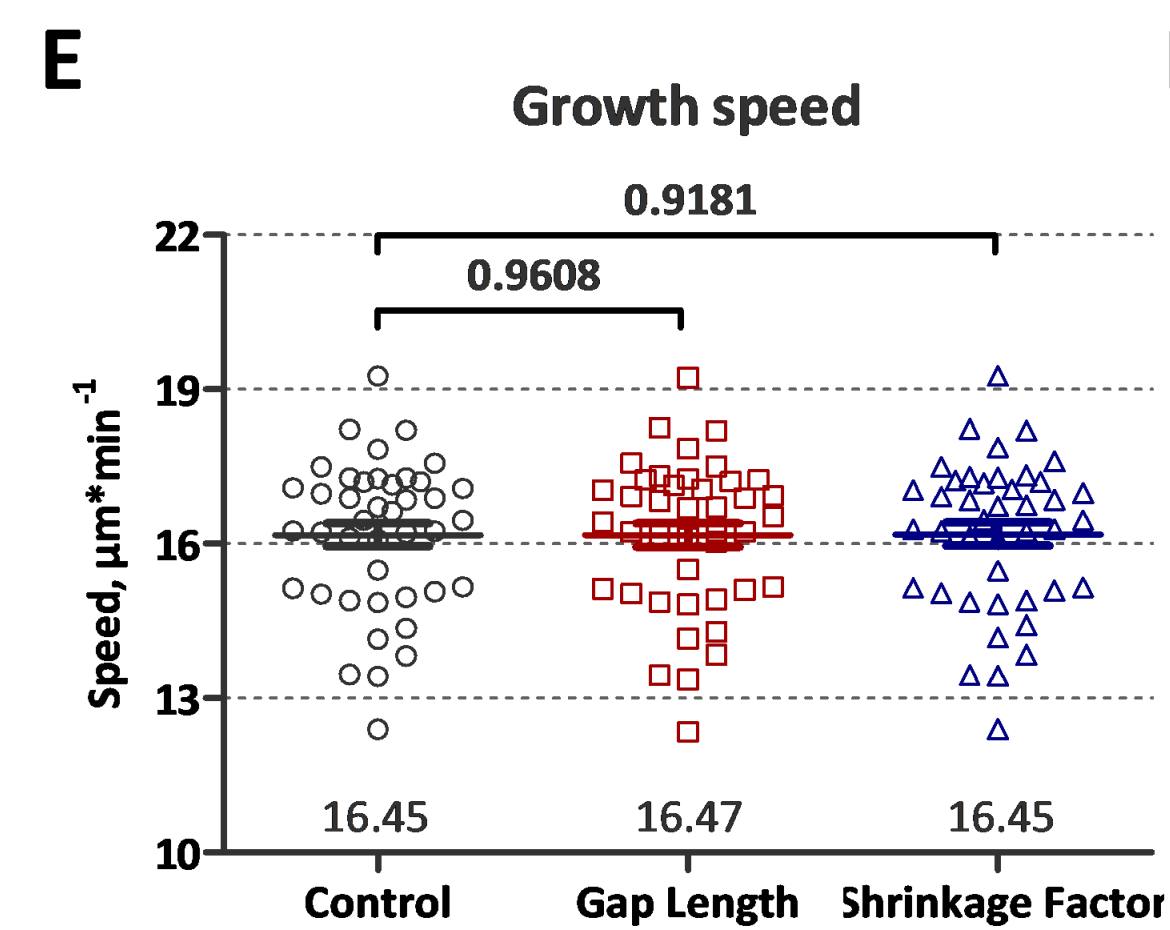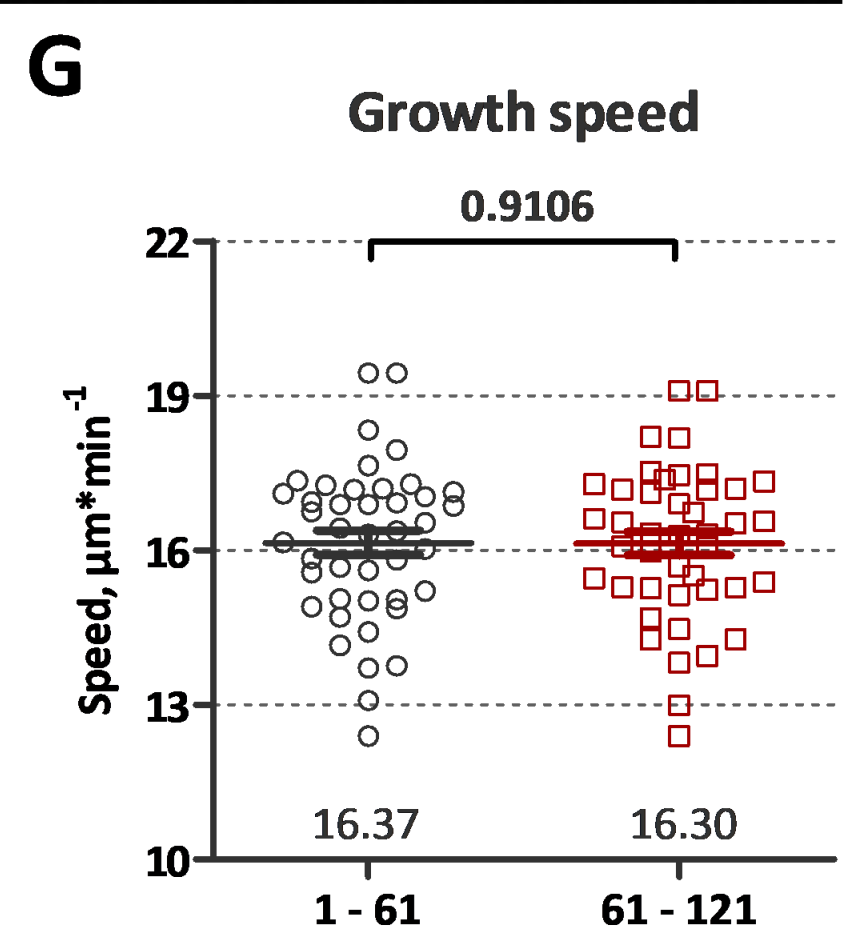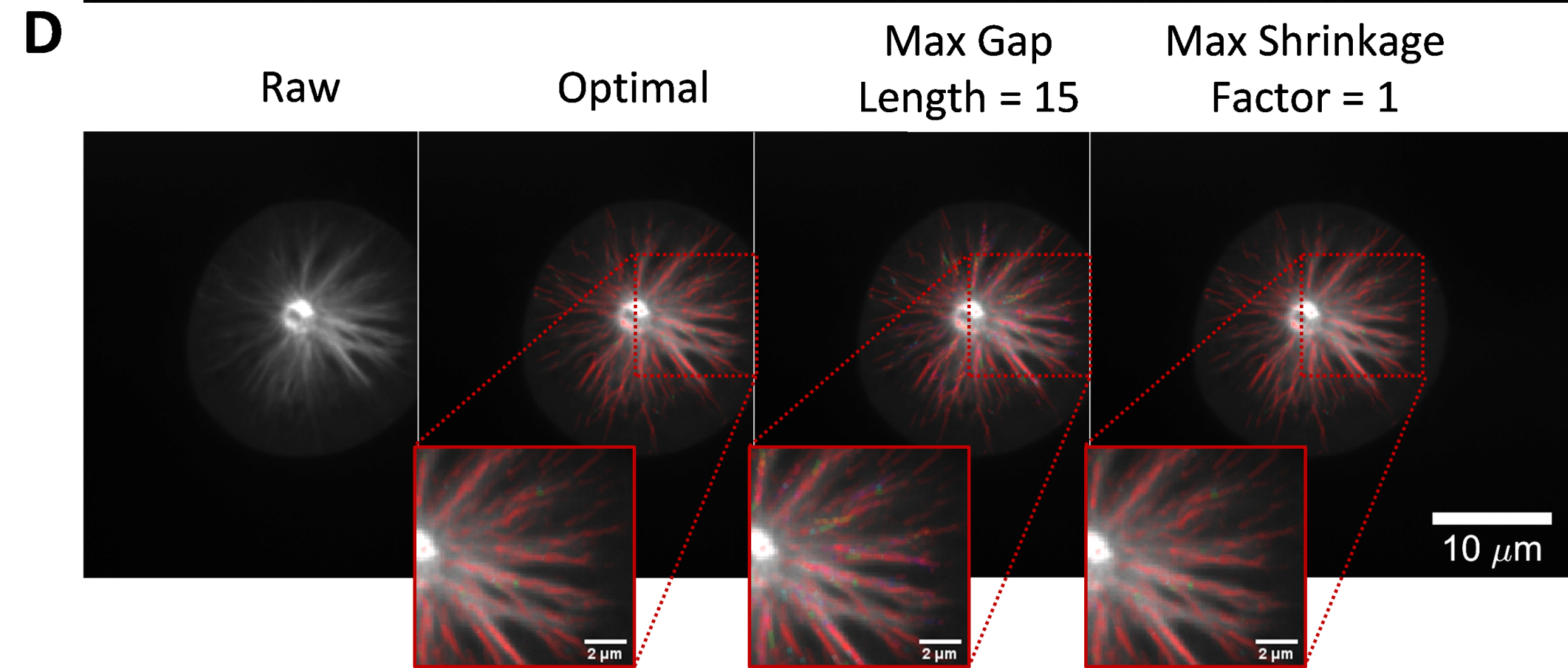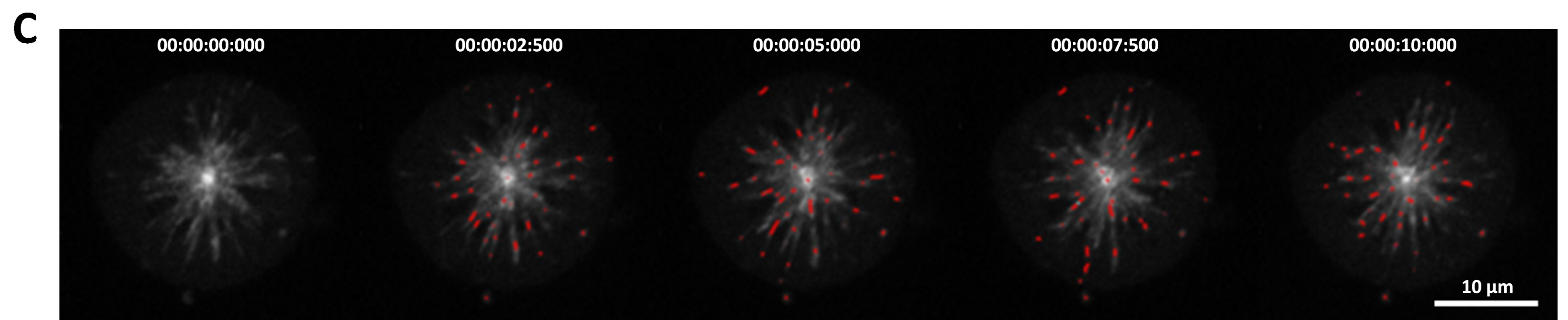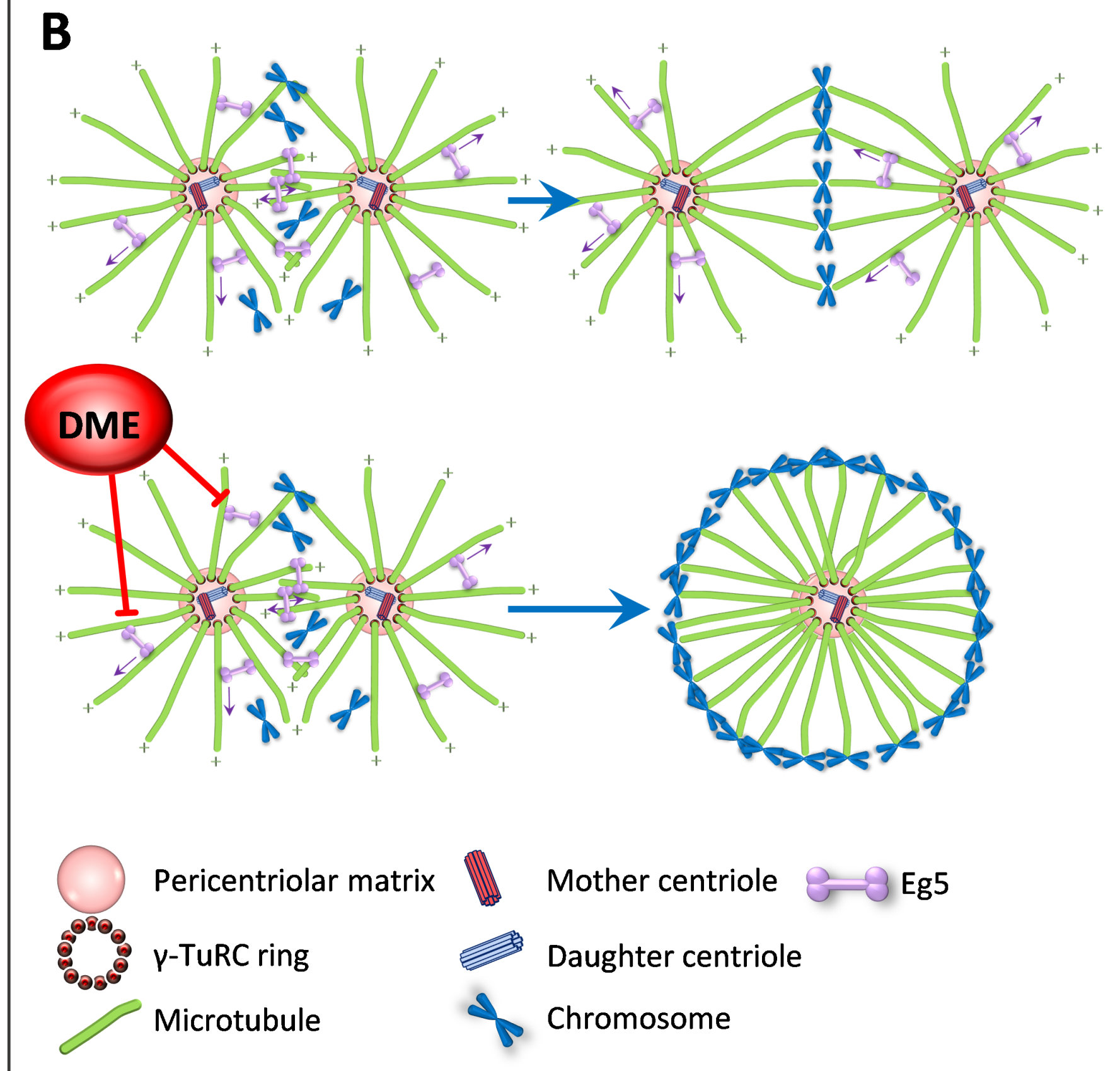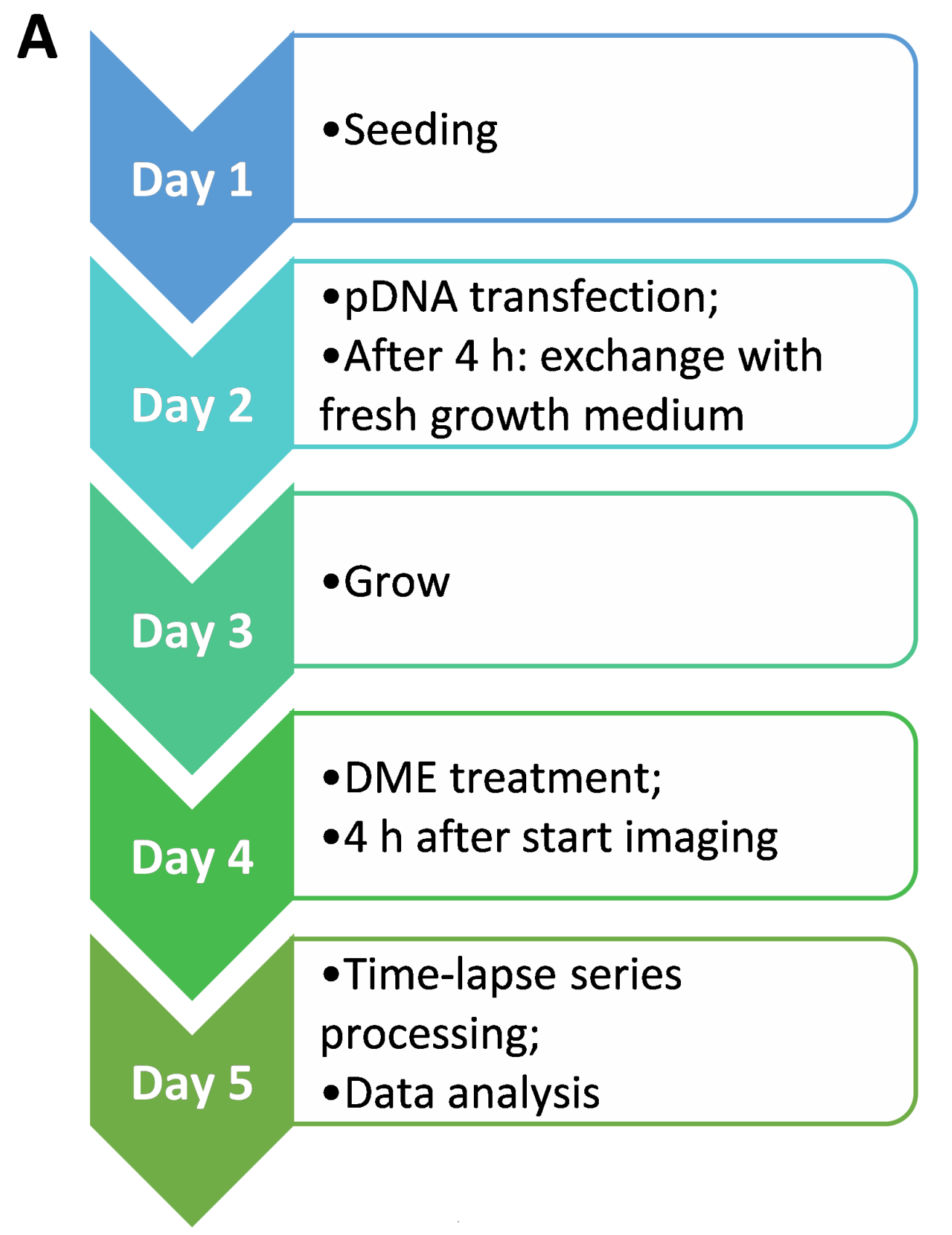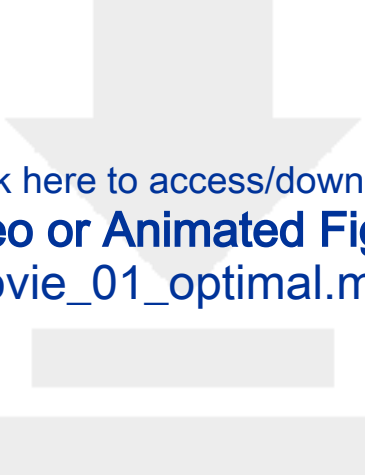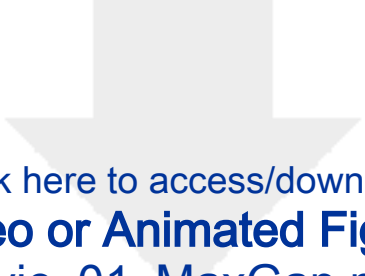
Figure 1

Video 1

Click here to access/download
Video or Animated Figure
Movie_01_raw.mov

Click here to access/download
Video or Animated Figure
Movie_01_optimal.mov

Video 3
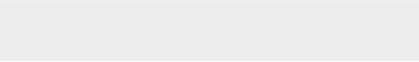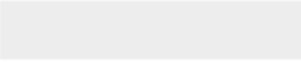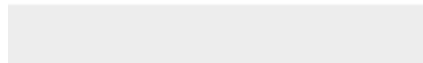
Click here to access/download
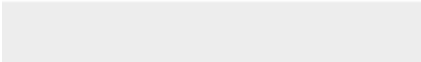**Video or Animated Figure**
Movie_01_MaxGap.mov

Click here to access/download
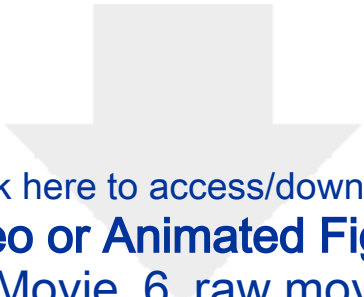
Video or Animated Figure

Movie_01_Shrinkage.mov

Click here to access/download

Video or Animated Figure

Movie_6.mov

Video 6

Click here to access/download
Video or Animated Figure
Movie_6_raw.mov
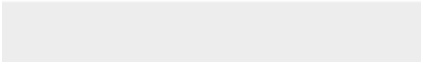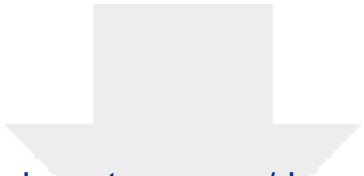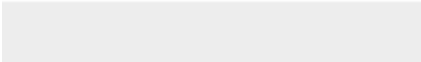
Click here to access/download
Video or Animated Figure
Movie_7.mov

Click here to access/download

Video or Animated Figure

Movie_7_raw.mov

Name of Material/ Equipment	Company
Dimethylenastron	Merck
DMEM w/o phenol red	Gibco
DPBS	Gibco
Fetal bovine serum	Biochrom
Fibronectin Bovine Plasma	Merck
GlutaMAX	Gibco
jetPRIME	Polyplus
EB3-TdTomato	Addgene
RPMI 1640	Gibco
Trypan Blue	Merck
Trypsin/EDTA solution	Biochrom
μ-slide	Ibidi
Eclipse Ti Inverted microscope	Nikon
Objective	Nikon
ACAL Laser Excahnger	Nikon
Spinning disk module	Andor
Camera	Andor
Environmental Chamber	Okolab
HeLa Cells	DSMZ
NIS Elements v4	Nikon
MATLAB	Mathworks

Prism 8   GraphPad

Catalog Number	Comments/Description
324622	
31053-28	
14190-094	
S0415	
F4759	Sterile powder
35050-038	Stable glutamine substitutive
114-15	
plasmid #50708	
61870-010	
T8154-20ML	
L2143	0.05% / o.02 % w/o calcium and magnesi
80426	4-well slide with #1.5 coverslip
NA	
MRD01991	CFI Apo TIRF 100XC Oil
	Laser box. 405, 458, 488, 514, 561 and 6
CSU-W	
iXon Ultra 888	
	Dark chamber equipped with CO2 supply
ACC-57	
	Spinning disk microscope. Acquisition So
	Computing environment

Statistical analysis and display software

ium

47nm

, tmeperature control and humidifier

ftware

jove
JOURNAL OF
VISUALIZED EXPERIMENTS

1 Alewife Center #200
Cambridge, MA 02140
tel. 617.945.9051
www.jove.com

ARTICLE AND VIDEO LICENSE AGREEMENT

Title of Article:	Measurement of microtubule dynamics by spinning disk microscopy in live cells synchronized at prophase.
Author(s):	Naira Movsisyan, Luis A. Pardo

Item 1: The Author elects to have the Materials be made available (as described at http://www.jove.com/publish) via:

🚫 Standard Access ☐ Open Access

Item 2: Please select one of the following items:

🚫 The Author is **NOT** a United States government employee.

☐ The Author is a United States government employee and the Materials were prepared in the course of his or her duties as a United States government employee.

☐ The Author is a United States government employee but the Materials were NOT prepared in the course of his or her duties as a United States government employee.

ARTICLE AND VIDEO LICENSE AGREEMENT

1.   **Defined Terms.** As used in this Article and Video License Agreement, the following terms shall have the following meanings: "**Agreement**" means this Article and Video License Agreement; "**Article**" means the article specified on the last page of this Agreement, including any associated materials such as texts, figures, tables, artwork, abstracts, or summaries contained therein; "**Author**" means the author who is a signatory to this Agreement; "**Collective Work**" means a work, such as a periodical issue, anthology or encyclopedia, in which the Materials in their entirety in unmodified form, along with a number of other contributions, constituting separate and independent works in themselves, are assembled into a collective whole; "**CRC License**" means the Creative Commons Attribution-Non Commercial-No Derivs 3.0 Unported Agreement, the terms and conditions of which can be found at: http://creativecommons.org/licenses/by-nc-nd/3.0/legalcode; "**Derivative Work**" means a work based upon the Materials or upon the Materials and other pre-existing works, such as a translation, musical arrangement, dramatization, fictionalization, motion picture version, sound recording, art reproduction, abridgment, condensation, or any other form in which the Materials may be recast, transformed, or adapted; "**Institution**" means the institution, listed on the last page of this Agreement, by which the Author was employed at the time of the creation of the Materials; "**JoVE**" means MyJove Corporation, a Massachusetts corporation and the publisher of The Journal of Visualized Experiments; "**Materials**" means the Article and / or the Video; "**Parties**" means the Author and JoVE; "**Video**" means any video(s) made by the Author, alone or in conjunction with any other parties, or by JoVE or its affiliates or agents, individually or in collaboration with the Author or any other parties, incorporating all or any portion of the Article, and in which the Author may or may not appear.

2.   **Background.** The Author, who is the author of the Article, in order to ensure the dissemination and protection of the Article, desires to have the JoVE publish the Article and create and transmit videos based on the Article. In furtherance of such goals, the Parties desire to memorialize in this Agreement the respective rights of each Party in and to the Article and the Video.

3.   **Grant of Rights in Article.** In consideration of JoVE agreeing to publish the Article, the Author hereby grants to JoVE, subject to **Sections 4** and **7** below, the exclusive, royalty-free, perpetual (for the full term of copyright in the Article, including any extensions thereto) license (a) to publish, reproduce, distribute, display and store the Article in all forms, formats and media whether now known or hereafter developed (including without limitation in print, digital and electronic form) throughout the world, (b) to translate the Article into other languages, create adaptations, summaries or extracts of the Article or other Derivative Works (including, without limitation, the Video) or Collective Works based on all or any portion of the Article and exercise all of the rights set forth in (a) above in such translations, adaptations, summaries, extracts, Derivative Works or Collective Works and(c) to license others to do any or all of the above. The foregoing rights may be exercised in all media and formats, whether now known or hereafter devised, and include the right to make such modifications as are technically necessary to exercise the rights in other media and formats. If the "Open Access" box has been checked in **Item 1** above, JoVE and the Author hereby grant to the public all such rights in the Article as provided in, but subject to all limitations and requirements set forth in, the CRC License.

4.   **Retention of Rights in Article.** Notwithstanding the exclusive license granted to JoVE in **Section 3** above, the Author shall, with respect to the Article, retain the non-exclusive right to use all or part of the Article for the non-commercial purpose of giving lectures, presentations or teaching classes, and to post a copy of the Article on the Institution's website or the Author's personal website, in each case provided that a link to the Article on the JoVE website is provided and notice of JoVE's copyright in the Article is included. All non-copyright intellectual property rights in and to the Article, such as patent rights, shall remain with the Author.

5.   **Grant of Rights in Video – Standard Access.** This **Section 5** applies if the "Standard Access" box has been checked in **Item 1** above or if no box has been checked in **Item 1** above. In consideration of JoVE agreeing to produce, display or otherwise assist with the Video, the Author hereby acknowledges and agrees that, Subject to **Section 7** below, JoVE is and shall be the sole and exclusive owner of all rights of any nature, including, without limitation, all copyrights, in and to the Video. To the extent that, by law, the Author is deemed, now or at any time in the future, to have any rights of any nature in or to the Video, the Author hereby disclaims all such rights and transfers all such rights to JoVE.

6.   **Grant of Rights in Video – Open Access.** This **Section 6** applies only if the "Open Access" box has been checked in **Item 1** above. In consideration of JoVE agreeing to produce, display or otherwise assist with the Video, the Author hereby grants to JoVE, subject to **Section 7** below, the exclusive, royalty-free, perpetual (for the full term of copyright in the Article, including any extensions thereto) license (a) to publish, reproduce, distribute, display and store the Video in all forms, formats and media whether now known or hereafter developed (including without limitation in print, digital and electronic form) throughout the world, (b) to translate the Video into other languages, create adaptations, summaries or extracts of the Video or other Derivative Works or Collective Works based on all or any portion of the Video and exercise all of the rights set forth in (a) above in such translations, adaptations, summaries, extracts, Derivative Works or Collective Works and (c) to license others to do any or all of the above. The foregoing rights may be exercised in all media and formats, whether now known or hereafter devised, and include the right to make such modifications as are technically necessary to exercise the rights in other media and formats. For any Video to which this **Section 6** is applicable, JoVE and the Author hereby grant to the public all such rights in the Video as provided in, but subject to all limitations and requirements set forth in, the CRC License.

7.   **Government Employees.** If the Author is a United States government employee and the Article was prepared in the course of his or her duties as a United States government employee, as indicated in **Item 2** above, and any of the licenses or grants granted by the Author hereunder exceed the scope of the 17 U.S.C. 403, then the rights granted hereunder shall be limited to the maximum rights permitted under such statute. In such case, all provisions contained herein that are not in conflict with such statute shall remain in full force and effect, and all provisions contained herein that do so conflict shall be deemed to be amended so as to provide to JoVE the maximum rights permissible within such statute.

8.   **Protection of the Work.** The Author(s) authorize JoVE to take steps in the Author(s) name and on their behalf if JoVE believes some third party could be infringing or might infringe the copyright of either the Author's Article and/or Video.

9.   **Likeness, Privacy, Personality.** The Author hereby grants JoVE the right to use the Author's name, voice, likeness, picture, photograph, image, biography and performance in any way, commercial or otherwise, in connection with the Materials and the sale, promotion and distribution thereof. The Author hereby waives any and all rights he or she may have, relating to his or her appearance in the Video or otherwise relating to the Materials, under all applicable privacy, likeness, personality or similar laws.

10.   **Author Warranties.** The Author represents and warrants that the Article is original, that it has not been published, that the copyright interest is owned by the Author (or, if more than one author is listed at the beginning of this Agreement, by such authors collectively) and has not been assigned, licensed, or otherwise transferred to any other party. The Author represents and warrants that the author(s) listed at the top of this Agreement are the only authors of the Materials. If more than one author is listed at the top of this Agreement and if any such author has not entered into a separate Article and Video License Agreement with JoVE relating to the Materials, the Author represents and warrants that the Author has been authorized by each of the other such authors to execute this Agreement on his or her behalf and to bind him or her with respect to the terms of this Agreement as if each of them had been a party hereto as an Author. The Author warrants that the use, reproduction, distribution, public or private performance or display, and/or modification of all or any portion of the Materials does not and will not violate, infringe and/or misappropriate the patent, trademark, intellectual property or other rights of any third party. The Author represents and warrants that it has and will continue to comply with all government, institutional and other regulations, including, without limitation all institutional, laboratory, hospital, ethical, human and animal treatment, privacy, and all other rules, regulations, laws, procedures or guidelines, applicable to the Materials, and that all research involving human and animal subjects has been approved by the Author's relevant institutional review board.

11.   **JoVE Discretion.** If the Author requests the assistance of JoVE in producing the Video in the Author's facility, the Author shall ensure that the presence of JoVE employees, agents or independent contractors is in accordance with the relevant regulations of the Author's institution. If more than one author is listed at the beginning of this Agreement, JoVE may, in its sole

![jove logo] JOURNAL OF VISUALIZED EXPERIMENTS

1 Alewife Center #200
Cambridge, MA 02140
tel. 617.945.9051
www.jove.com

ARTICLE AND VIDEO LICENSE AGREEMENT

discretion, elect not take any action with respect to the Article until such time as it has received complete, executed Article and Video License Agreements from each such author. JoVE reserves the right, in its absolute and sole discretion and without giving any reason therefore, to accept or decline any work submitted to JoVE. JoVE and its employees, agents and independent contractors shall have full, unfettered access to the facilities of the Author or of the Author's institution as necessary to make the Video, whether actually published or not. JoVE has sole discretion as to the method of making and publishing the Materials, including, without limitation, to all decisions regarding editing, lighting, filming, timing of publication, if any, length, quality, content and the like.

12.   **Indemnification.** The Author agrees to indemnify JoVE and/or its successors and assigns from and against any and all claims, costs, and expenses, including attorney's fees, arising out of any breach of any warranty or other representations contained herein. The Author further agrees to indemnify and hold harmless JoVE from and against any and all claims, costs, and expenses, including attorney's fees, resulting from the breach by the Author of any representation or warranty contained herein or from allegations or instances of violation of intellectual property rights, damage to the Author's or the Author's institution's facilities, fraud, libel, defamation, research, equipment, experiments, property damage, personal injury, violations of institutional, laboratory, hospital, ethical, human and animal treatment, privacy or other rules, regulations, laws, procedures or guidelines, liabilities and other losses or damages related in any way to the submission of work to JoVE, making of videos by JoVE, or publication in JoVE or elsewhere by JoVE. The Author shall be responsible for, and shall hold JoVE harmless from, damages caused by lack of sterilization, lack of cleanliness or by contamination due to

the making of a video by JoVE its employees, agents or independent contractors. All sterilization, cleanliness or decontamination procedures shall be solely the responsibility of the Author and shall be undertaken at the Author's expense. All indemnifications provided herein shall include JoVE's attorney's fees and costs related to said losses or damages. Such indemnification and holding harmless shall include such losses or damages incurred by, or in connection with, acts or omissions of JoVE, its employees, agents or independent contractors.

13.   **Fees.** To cover the cost incurred for publication, JoVE must receive payment before production and publication the Materials. Payment is due in 21 days of invoice. Should the Materials not be published due to an editorial or production decision, these funds will be returned to the Author. Withdrawal by the Author of any submitted Materials after final peer review approval will result in a US$1,200 fee to cover pre-production expenses incurred by JoVE. If payment is not received by the completion of filming, production and publication of the Materials will be suspended until payment is received.

14.   **Transfer, Governing Law.** This Agreement may be assigned by JoVE and shall inure to the benefits of any of JoVE's successors and assignees. This Agreement shall be governed and construed by the internal laws of the Commonwealth of Massachusetts without giving effect to any conflict of law provision thereunder. This Agreement may be executed in counterparts, each of which shall be deemed an original, but all of which together shall be deemed to me one and the same agreement. A signed copy of this Agreement delivered by facsimile, e-mail or other means of electronic transmission shall be deemed to have the same legal effect as delivery of an original signed copy of this Agreement.

A signed copy of this document must be sent with all new submissions. Only one Agreement is required per submission.

CORRESPONDING AUTHOR

Name: Luis A. Pardo

Department: AG Oncophysiology

Institution: Max-Planck-Institute of Experimental Medicine

Title: Research Group Leader

Signature: _[signature]_ Digitally signed by Luis A. Pardo
Date: 2019.06.25 14:41:59 +02'00'

Date: June 25, 2019

Please submit a **signed** and **dated** copy of this license by one of the following three methods:
1. Upload an electronic version on the JoVE submission site
2. Fax the document to +1.866.381.2236
3. Mail the document to JoVE / Attn: JoVE Editorial / 1 Alewife Center #200 / Cambridge, MA 02140

Dear Editors,

Thank you very much for handling our submission. We also wish to thank the reviewers for their helpful comments.

Enclosed please find a revised version of the manuscript, where we have responded to the editorial and reviewer requests and comments. A detailed response to the reviewers follows.

Reviewer #1:

Manuscript Summary:

The manuscript describes a method to track growing microtubule ends in monopolar spindles generated by treating HeLa cells with Dimethylenastron, an Eg5 inhibitor. Timelapse data are obtained using spinning disk microscopy in a single plane of cells transiently transfected with EB3-tdTomato. The analysis is using u-track, a MATLAB-based open source software by the Danuser lab. Therefore, the title is misleading and should better reflect what the method actually shows: e.g. "Measurement of microtubule assembly by spinning disk microscopy in monopolar spindles"

Thank you very much for this comment. The title is more accurate this way. We have kept the word "dynamics" instead of "assembly" because we believe it is also more accurate. The title reads now: "Measurement of microtubule dynamics by spinning disk microscopy in monopolar mitotic spindles".

Major Concerns:

The method described has major limitations, the discussion of which is missing from the manuscript.

1. Using a marker for growing plus ends limits the analysis to microtubule assembly speed rather than the full set of microtubule dynamics parameters.

We agree that the method measures only growth events directly. Nevertheless, the subsequent anlaysis extrapolates the information on the pause and shrinkage events by linking sequential growth phases meeting certain criteria. The reconstruction of full trajectories [1,2] is based on the spatially and temporally global tracking framework [3]. This has been now clearly stated in the revised manuscript: "Although the plus end binding proteins trace only MT growth phases, the U-Track v2.2.0 extrapolates the information on the pause and shrinkage events by linking sequential growth phases and reconstructing the full trajectories [26,50]. The algorithm is based on the spatially and temporally global tracking framework described by Jaqaman et al. [51]" (lines 324-351).

2. Arresting cells with an Eg5 inhibitor does not result in prophase cells, but a prometaphase-like state. How comparable microtubule dynamics measured in these arrested cells versus cycling cells in prometaphase is unclear and not discussed.

Thank you for pointing this out. We have corrected the definition of the phase of arrest. Other than that, it has been shown that arrest of cells at prometaphase with Eg5 inhibitor monastrol and its derivatives, such as dimethylenastron, does not affect microtubule dynamics [4-6]. We have explicitly included this information: "Inhibition of cells at prometaphase with the Eg5 inhibitor DME and other monastrol derivatives does not affect microtubule dynamics[43-45], which makes DME a useful tool for studying MT dynamics both in fixed and live cells[44]" (lines 108-109).

3. Imaging in a single plane is a severe limitation to obtaining any useful information about the lifetime of assembly events. This can be overcome by rapid volume imaging using lattice light sheet microscopy, which is far superior to spinning disk confocal imaging hailed as the best available in the manuscript. A fine example of plus tip tracking in 3D in cycling mitotic cells is here (DOI: 10.1117/1.JBO.20.10.101206) and the authors should cite it and compare their data to the data obtained for prometaphase cells therein.

The lattice light-sheet microscopy approach is indeed superior, but it is still less generally available than spinning disk, and requires much more time and computer power, as pointed out by Yamashita et al. in the manuscript the reviewer suggested. We have been more explicit and clarified that the method we describe is not the best available, but is in comparison more accessible. "Recently, the combination of lattice light-sheet microscopy of a mitotic spindle at sub-second intervals, together with sophisticated image processing allows the analysis of MT assembly rates in three-dimensions[63,64]. This has obvious advantages over CLSM, but further improvements will be required before the method becomes of general use, such as the expansion of strategies used in U-Track to the third dimension[26,50,63]" (lines. 480-484).

4. It is unclear to me why the authors choose to do a transient transfection in HeLa cells resulting in highly variable expression of EB3-tdTomato. Stable HeLa cell lines expressing EB3-tdTomato have been published previously and could have been obtained from the authors (for example DOI: 10.1038/ncb2297).

We use transient transfection for several reasons. First, we are anyhow transfecting the cells for our experiments. Furthermore, this allows us to be less worried about insertion artifacts, clonal enrichment and other problems of stable cell lines. At the same time, we typically obtain faint fluorescence in stable cell lines, unless we specifically select for cells highly expressing EB3, which would introduce a bias. Nevertheless, it could be very advantageous in other settings, and we state this in the new version of the manuscript. We discuss the possibility of using a cell line stably expressing EB3-tdTomato as a note in the protocol. "*Alternatively, a cell line stably expressing EB3-tdTomato can be used in the experiments; this should reduce variability in expression levels of EB3-tdTomato between preparations and between cells from the same preparation[49]*" (lines 188-190).

5. Further, the authors should test how robust their method really is and how much damage the cell experiences during imaging. A possible way to demonstrate this, is to compare microtubule assembly speed in the first half of the movie versus the second half of the movie and show that resulting data are not significantly different from each other. Another test for robustness is how well the tracking works for different intensity images. It would be good to show an overlay of the time projection of the movie and the actual tracks as it would allow the reader to judge whether the tracking is faithful. The authors suggest to use the same parameters for the entire dataset, so the tracking should be shown for a low-expressing and a high-expressing cell across the range they suggest suitable for the experiment.

Thank you for pointing this out. We have now added three additional points in Figure 1 (D, G and H). Firstly, in Figure 1, D we included time projection images of the time-lapse movies before and after tracking for the suggested optimal conditions, and for each of the parameters discussed. Secondly, we compared the two halves of the movies and growth speed mean (Figure 1, G) and dynamicity (Figure 1,H) values are plotted. There were no significant differences between the two halves. For readers to get the impression on which kind of cells should not be included in the analysis, we included additional videos (Videos 7 and 8).

Minor Concerns:

The method is of limited use as it is described for a specific model of microscope and proprietary imaging format. It would be good if the authors would comment on how other formats of imaging data could be integrated into the same pipeline.

We have described the method for our particular system, which is what will be shown in the video. The software we suggest uses Bio-Formats image importer, which allows to import and analyse virtually any image format. *"The U-Track software is compatible with other image data formats; it uses Bio-Formats, which recognises different life science data formats[53]" (Lines 251-252).*

Reviewer #2:

Manuscript Summary:

In this manuscript the author present a modified protocol for measuring microtubule dynamics in Prophase arrested HeLa cells using spinning disk microscopy. They highlight the advantage of spinning disk laser scanning microscope over confocal laser scanning microscope in terms of fast imaging with high signal to noise ratio. The authors overexpressed td-tomato-labeled EB3 protein in HeLa cells to study MT plus-end assembly rates. The author claims that tdTomato fluorescent protein has improved brightness and photostability in comparison to the EGFP and tdTomato require less laser power for excitation thus improving resolution and postprocessing during MT dynamics analysis.

Major Concerns:

1. The paper lacks a clear biological statement/question.

Since we describe a method rather than answering an exact biological question, we give only a very general background on the importance of microtubule dynamics analysis (lines 53-62).

2. The authors do not actually show that the spinning disk or the FP led to decreased phototoxicity. It is an assumption. For example, they should compare and analyze the expression of both td tomato and EGFP constructs. Also, did the author encounter the problem of aggregation of td tomato? The cell debris they refer in supplemental movie 5 might be aggregation.

Thank you very much for your comment. We however respectfully disagree. It is a well established fact that phototoxicity is directly proportional to the energy delivered [8-11], which is lower in spinning disk microscopy (compared to laser scanning) and also lower the longer the excitation wavelength. The effect of blue light, in particular on cell division has also been described [8]. We did not encounter aggregation of tdTomato, and this can be due to the low levels of expression we intentionally use (please see response to comment #4 from reviewer 1). This gives us the possibility to identify dynamic microtubules. Nevertheless, the MT tracking software also limits the analysis only to certain particle size.

3. It is hard to understanding the terms used in Figure 1D and E. Figures 1D & E show that the two factors (viz. 'maximum gap length' and 'maximum shrinkage factor') do not change the growth speed analysis but affect the dynamicity analysis. However, the values of these parameters/factors are not mentioned properly. Please mention these values for the three cases presented in the figure. It is also surprising to see that these two parameters do not have any effect on the growth speed because the values for these three cases presented in Figure 1D are identical.

The growth speed is derived from the sub-tracks and, therefore, it is not affected by the parameters, such as "Maximum Gap Length" and "Maximum Shrinkage Factor", whereas dynamicity defined as "collective displacement of all gap-containing tracks over their collective lifetimes" will be affected the most. "Maximum Gap Length" defines the number of frames after or before the current frame which will still be considered as part of one MT trajectory, whereas "Maximum Shrinkage Factor" shows times difference of shrinkage speed compared to the growth speed. Therefore, collectively these two parameters will define the size and duration of the "gap". In other words, these two parameters are required for reconstructing the full trajectory with all the "gap" events in it, and thus influencing only the dynamicity, but not the growth speed.

4. The authors pointed out that "the sensitivity and accuracy of the analysis are strongly dependent on several aspects". However, the authors should specifically mention some of these "aspects".

Thank you for pointing this omission out. We have now defined which "aspects" we were referring to.

5. The authors need to show how the other parameters of the U-Track software, such as thresholding parameters, maximum forward angle to link the tracks etc. alter the results.

The reviewer is right that this is a very important information. However, we are just users of the software, and left those definitions to the actual creators of the tool. We are merely combining already established methods with spinning disk confocal microscopy and the use of a red fluorescent probe, and we refer the readers to the documentation of the software and original publications where all the parameters are described and explained in great detail.

Minor Concerns:

1. What laser powers were used?

The imaging was performed at a laser power of 5.3 mW and 100 ms exposure time with the shutter closed between the time intervals. We now mention this on lines 221-222.

3. Detail about statistical analysis should also be mentioned in point 5, line 237.

Thank you for pointing this out. We have added the information. "The m-files contain statistical information (median, mean and standard deviation) on different parameters, such as growth speed, MT dynamicity, etc. The detailed list of the parameters is given in the technical report provided with the previous version of the software, plusTipTracker[50,52]" (lines 303-308)

1   Applegate, K. T. *et al.* plusTipTracker: Quantitative image analysis software for the measurement of microtubule dynamics. *J Struct Biol.* **176** (2), 168-184, (2011).

2   Matov, A. *et al.* Analysis of microtubule dynamic instability using a plus-end growth marker. *Nat Methods.* **7** (9), 761-768, (2010).

3   Jaqaman, K. *et al.* Robust single-particle tracking in live-cell time-lapse sequences. *Nat Methods.* **5** (8), 695-702, (2008).

4   Kapoor, T. M., Mayer, T. U., Coughlin, M. L. & Mitchison, T. J. Probing spindle assembly mechanisms with monastrol, a small molecule inhibitor of the mitotic kinesin, Eg5. *The Journal of Cell Biology.* **150** (5), 975-988, (2000).

5   Ertych, N. *et al.* Increased microtubule assembly rates influence chromosomal instability in colorectal cancer cells. *Nat Cell Biol.* **16** (8), 779-791, (2014).

6   Brito, D. A., Yang, Z. & Rieder, C. L. Microtubules do not promote mitotic slippage when the spindle assembly checkpoint cannot be satisfied. *The Journal of Cell Biology.* **182** (4), 623-629, (2008).

7   Shaner, N. C., Patterson, G. H. & Davidson, M. W. Advances in fluorescent protein technology. *Journal of Cell Science.* **120** (24), 4247-4260, (2007).

8   Laissue, P. P., Alghamdi, R. A., Tomancak, P., Reynaud, E. G. & Shroff, H. Assessing phototoxicity in live fluorescence imaging. *Nature Methods.* **14** 657, (2017).

9   Magidson, V. & Khodjakov, A. Circumventing photodamage in live-cell microscopy. *Methods in cell biology.* **114** 545-560, (2013).

10   Douthwright, S. & Sluder, G. Live Cell Imaging: Assessing the Phototoxicity of 488 and 546 nm Light and Methods to Alleviate it. *Journal of Cellular Physiology.* **232** (9), 2461-2468, (2017).

11   Icha, J., Weber, M., Waters, J. C. & Norden, C. Phototoxicity in live fluorescence microscopy, and how to avoid it. *Bioessays.* **39** (8), 1700003, (2017).

Editorial comments.

We have edited the revised manuscript to remove any commercial names, and addet titles to the video files.

We have uploaded the revised figure in .ai format.